Temperature Dependence of Quantum Dots-In-Well Infrared Photo Detectors (QDIPs) using Photoluminescence

Noor H Jabarullah

***Abstract:** A research of quantity dots-in-well infrared photo detectors (QDIPs) produces helpful outcomes for creating a two-color QDIP. Quantum dot infrared photo detectors (QDIPs) have been shown to be a main technology in mid-and long-wavelength infrared detection owing to their capacity for normal incidence operation and low dark current. This research explores infrared detectors based on intersubband transitions in a novel heterostructure of InAs / In0.15 Ga0.85 As / GaAs quantum dots-in-well (DWELL). The InAs quantum dots are also positioned in an In0.15 Ga0.85 in the DWELL framework, which in turn is well positioned with the In0.1Ga0.9As obstacle in GaAs quantum. Using fourier transform infrared spectroscopy, the optical characteristics of the sample were researched using photoluminescence and photocurrent. Spectrally adjustable reaction was noted at 6.2µm and 7.5µm with prejudice and lengthy wave IR reaction.*

I. INTRODUCTION

High performance infrared (IR) photodetection is desirable for many applications involving thermal imaging, chemical analysis, night vision, remote sensing, space range, mine detection and fiber optic communications. Depending on the implementation, one may want either distinct requirements, either a wide, multicolor response from the detector, or a sharp single wavelength reaction. In addition to generating pictures with some color depth, multicolor IR detection has the capacity to determine the observed body temperature, so it is much more advantageous for a particular imaging scheme. Multi-color focal plane array (FPA) photodetectors are particularly helpful for medical and military imaging as well as environmental monitoring applications.

Quantum dots-in-well DWELL is component of a fresh technology of nano-photonic semiconductor devices, using stacked layers of quantum dots (QDs) as the active region in their constructions. DWELL photodetectors are a promising fresh advance that will hopefully overcome many of the shortcomings of current IR photodetection technologies. QDIPs use inter-subband absorption to detect small absorption, 3-5µm & 8-14µm atmospheric' windows' medium and long wavelength light radiation.

Significant research has been carried out into the study of QDIPs, but little in the way of multi-color QDIP development, despite their desirability for a wide variety of applications. The objective of this project is to acquire the sample's optical properties through photoluminescence and photocurrent measurement while analyzing the benefits and disadvantages of the quantum-dots-in-well photodetector. This paper involves studying the mixture or hybrid of quantum-dot and quantum-well, known as dot-in-well (DWELL), and optimizing the benefits of the QDIP hypothesis by this hybrid system. The aim of this paper is to study the optical properties of the DWELL QDIP sample

using experimental techniques. The experimental work on this project focuses studying the optical properties by the means of photoluminescence and photocurrent.

II. ENERGY BAND STRUCTURE

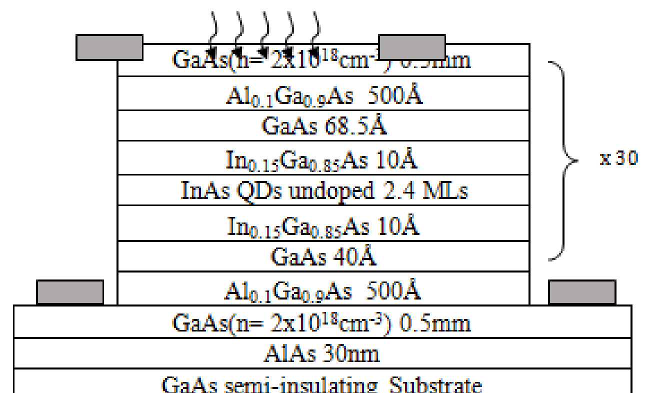

Fig. 1 Hetero structure of schematic of InAs/ $In_{0.15}Ga_{0.8}As$/GaAs dots-in-well infrared photo detector

Revised Manuscript Received on June 22, 2019.

Noor H Jabarullah, Universiti Kuala Lumpur, Malaysia Institute of Aviation Technology

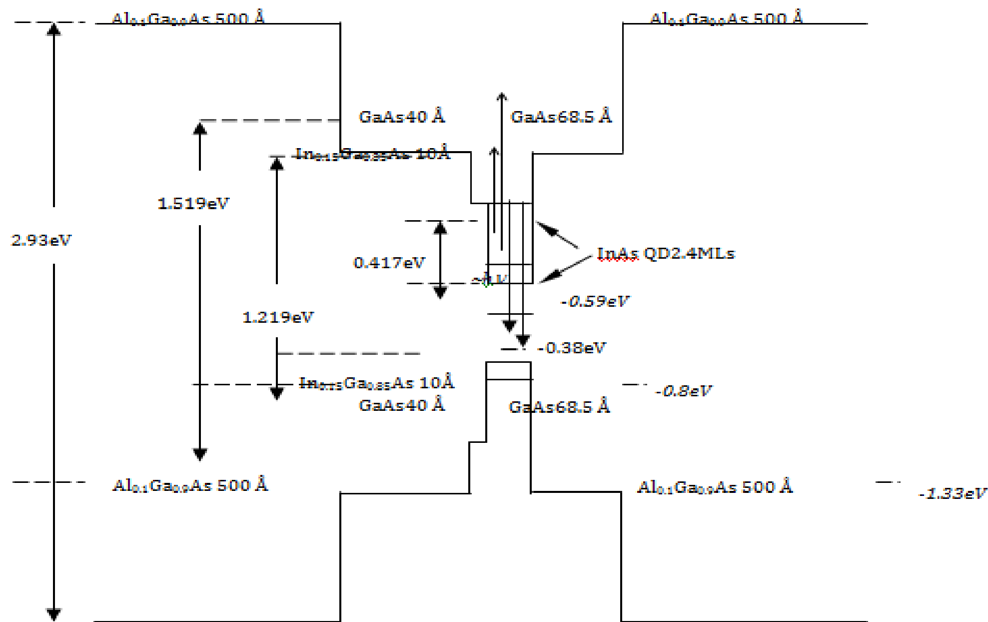

Fig. 2 The unstrained energy band structure

Figure 1 shows schematic of the DWELL structure and the energy band profile for the sample structure is illustrated in Figure 2. The valence band offset (VBO) of the $Al_{0.1}Ga_{0.9}As$, GaAs, $In_{0.15}Ga_{0.8}As$ and InAs is -1.33eV, -0.8eV, -0.38eV and -0.59eV respectively.

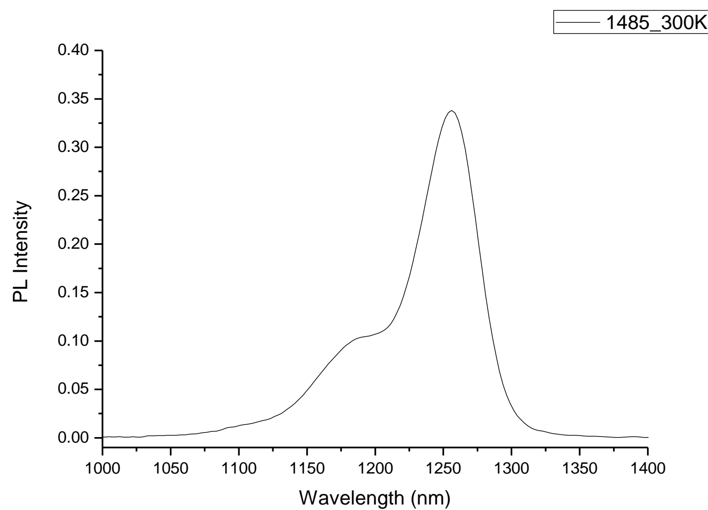

Fig. 3 Room temperature PL for the 30-period this InAs/ $In_{0.15}Ga_{0.8}As$/GaAs

The room temperature PL spectrum obtained from this InAs/ $In_{0.15}Ga_{0.8}As$/GaAs dots-in-well infrared photodetector QDIP is shown in Figure 3.13. The PL wavelength of the InAs is 1255nm showing that this device is crucial to achieve quantum efficiency without introducing dislocations.

Infrared photodetectors with an InAs/ $In_{0.15}Ga_{0.8}As$/GaAs DWELL active region suffer from strain related issues. Due to high compressive strain, a greater number of active region layers cannot be grown without introducing dislocations. More layers will enhance the absorption, which in turn increases the quantum efficiency,η of the photodetector. This increase in η will increase the responsivity and detectivity of the detectors.

In order to determine the energy levels it is necessary to include the effects due to strain on the structure. The energy values of the QW's are affected by the strain in the layers (Osbourn, 1982). GaAs has a direct energy gap at the Γ point of 1.519 and InAs has a direct energy gap of 0.417 at the Γ point. Thus the value of $In_{0.15}Ga_{0.8}As$ is less of GaAs and has been obtained from the ternary calculation depending on the alloy composition using a simple quadratic equation;

$$E_g(A_{1-x}B_x) = (1-x)E_g(A) + xE_g(B) + x(1-x)C \quad (3.1)$$

where C is the bowing parameters that has been obtained from linear interpolation between the two A and B binaries (Vurgaftman & Meyer, 2001).

The lattice mismatch between the substrate, the QWs and the other material in the sample is not too large, so when the mismatch is less than 7%, it is assumed that no misfits are generated at the interfaces by compression or expansion of the planes (Osbourn, 1982) and (Vurgaftman & Meyer, 2001). This means that the strain in the materials consist of uniform biaxial strain (hydrostatic) parallel to the interface and unaxial strain parallel to the growth direction. The hydrostatic component of compressive strain increases the bandgap and tensile strain reduces the bandgap. The strain effects not only on the band edges but also modifies the effective massed associated with the individual bands. The strained-induced of the bulk material responds to the shift of energies in QWs and barrier heights. The hydrostatic strain is obtained using below equation;

$$\varepsilon_{\parallel} = \varepsilon_{xx} = \varepsilon_{yy} = \frac{a_s - a_e}{a_e} \quad (3.2)$$

$$\varepsilon_{zz} = -2\frac{C_{12}}{C_{11}} \quad (3.3)$$

where ε_{xx}, ε_{yy} and ε_{zz} are diagonal strain components of strain tensor is defined to be negative for compressive strain. a_s is the lattice constant for the substrate and a_e, is the epilayer lattice constant. C_{12} and C_{11} is the elastic constants. The material parameters for the calculation of bandgap, VBO and strain are taken from Vurgaftman& Meyer (2001).

Energy bandgap change in the conduction band, ΔE_c and valence band, ΔE_v is given by;

$$\Delta E_c = a_c(\varepsilon_{xx} + \varepsilon_{yy} + \varepsilon_{zz}) \quad (3.4)$$

$$\Delta E_v = a_v(\varepsilon_{xx} + \varepsilon_{yy} + \varepsilon_{zz}) \quad (3.5)$$

From the Bir-Pikus strain interaction it is not sufficient to describe the full effect of the valence band strain. Shear deformation potential, b is necessary to explain the shear deformation that split the valence band into heavy/light hole.

The + and – signs refer to heavy and light hole respectively.

In order to calculate the ΔE_c and ΔE_v for the ternary materials linear interpolation between the binary data obtain from Vurgaftman & Meyer (2001) is used to determine the values if the parameters used.

It has been calculated that very small lattice constant difference between the substrate and the epilayer materials, very small strain value to the energy gap produced by the calculation. The QWs calculation was performed using formulas obtained from (Pryor & Pistol, 2005) and (Micaleff & Wiess, 1990) by PhD student in the group. The QDs strain can only be obtained using numerical calculation therefore, in this study values are obtained from numerical calculation using finite element method by PhD student in the group. Figure 3.14 shows the strained conduction band profile produced numerically.

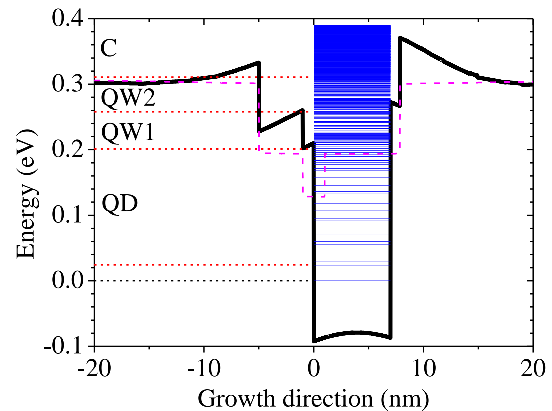

Fig. 3.14 The strained conduction band for InAs/ $In_{0.15}Ga_{0.8}As$/GaAs DWELL through the centre of the QD (solid line) and through the QW without crossing the dots (dashed line).

III. METHODOLOGY

Device fabrication

Device fabrication is done in a class-100 clean room in University of Sheffield where the 400μm x 400μm mesas were defined using photolithography, followed by metal evaporation and then etching techniques. The first stage was to define the mesa structure for the QDIPs using standard photolithography

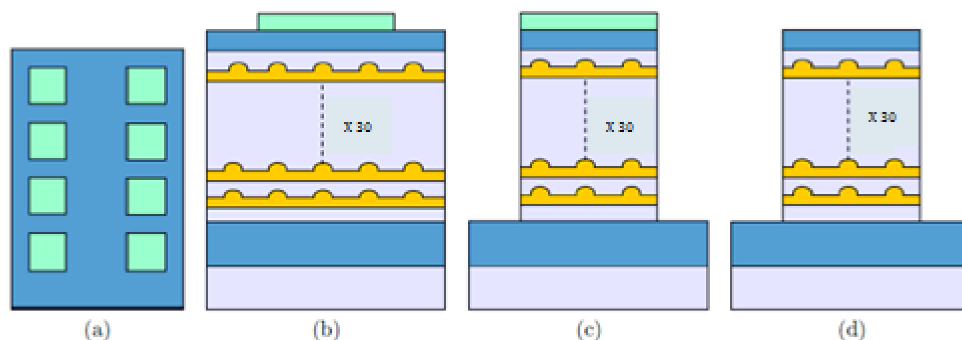

Fig. 4 The schematic of the mesa structure processes. (a) The top view of the patterned sample, with the photoresist marked in light blue. (b) The sample cross-section with the photoresist square on top. (c) Cross-section etching process. (d) A single mesa cross-section after photoresist been removed - reproduced from Sze & Ng(2007).

The second phase was the formation of metal contacts and the final packaging. Another photolithography step was taken to identify regions for metal contacts on the QDIPs. The lithography operation outlined in the above steps was repeated using a distinct metal contact mask. The pattern for the contacts was to leave transparent circles of 200µm diameter on top of each mesa and long transparent lines on the bottom contact layer, with the remainder of the collection covered in photoresist. This will allow each sample QDIP to have an autonomous top contact and a shared bottom contact. After the second photolithography phase, metal contacts were created first by washing the sample in HCl (10 percent) for 40s to remove natural oxidation. The technique of evaporation was placed for the n-type metal contacts using layers of Ge, Ni and Au. After that is the lift-off process by using acetone to remove the photoresist from the sample. The final step consists of annealing the contacts for 45 seconds using rapid thermal annealing under N2 flow at 400 ° C. The unit was lastly packaged by mounting it on a 12-pin TO5 header, as shown in Figure 3.7, with 25µm thick gold cables attached to the metal contacts on all the QDIPs in the sample, connecting them to the gold buttons on the header. This stage is essential to characterize the sample using photocurrent measurement.

Photoluminescence (PL) Measurement

Photoluminescence (PL) is the spontaneous emission of light from the optical excitation of a material used to explore the sample's optical properties. PL studies can be used to characterize both inherent electronic transitions and impurity electronic transitions as well as semiconductor and insulator defects. PL is the typical method used to characterize III-IV semiconductors owing to the benefit of non-destructive, non-electrical contact requiring minimal effort for sample preparing. PL detects the optical shift from an excited electronic state to lower electronic state, generally ground state (Figure 3.15). Due to fast thermalization, only transitions from the reduced electronic states can usually be noted at low temperatures. Most of the light outcomes from the excited electron's energy difference returning to its ground state.

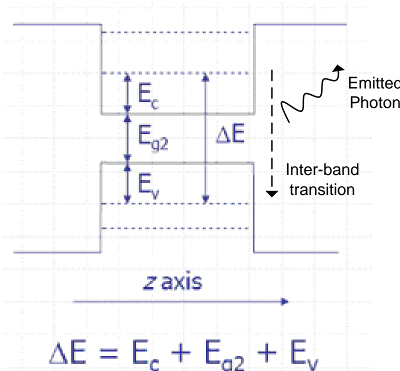

Fig. 5 Photoluminescence mechanism and relationship with electronic band structure

The PL spectra have narrow band which makes the analysis possible (Strading & Klipstein, 1990). The position of PL peaks is related to the energy of each excited level and can be used as sensitive probe to find impurities and other defects in semiconductors. The PL intensity can give more information on the quality of interfaces and surfaces. PL spectrum and the dependencies on its intensity on the irradiation intensity and device temperature provide important information for device characterisation. PL spectra and the intensity can be used determine the energy gap or wavelength of maximum gain, understand the component of ternary/quaternary layers its impurity levels and allows for the understanding and investigations of the recombination mechanism investigations (Gfroerer, 2000)

The PL measurement were completed using a Fourier Transform Infrared (FTIR) spectroscopy, FTIR is an efficient and dynamic technique that provides qualitative and quantitative information which require a broadband range from Near-IR to Far-IR spectrum. FTIR spectrometer collects and examines all wavelengths simultaneously instead of viewing each one separately. This technique is known as Felgett or multiplex advantage. The interferometer will produce infrared spectra by collecting the interferogram of a sample that involves Fourier Transform mathematical manipulation that can involve phase correction and apodization.

Photocurrent (PC) Measurement

In contrast to other absorption-like spectroscopy, photocurrent (PC) is a comparatively simple, fast and easy to acquired technique, which reveals clear and unambiguous excitonic absorptions of self-assembled QDs. In the PC spectroscopy, the undergone processes of the photogenerated carriers are complementary to the PL measurements.

IV. RESULTS AND DISCUSSIONS

Temperature Dependence

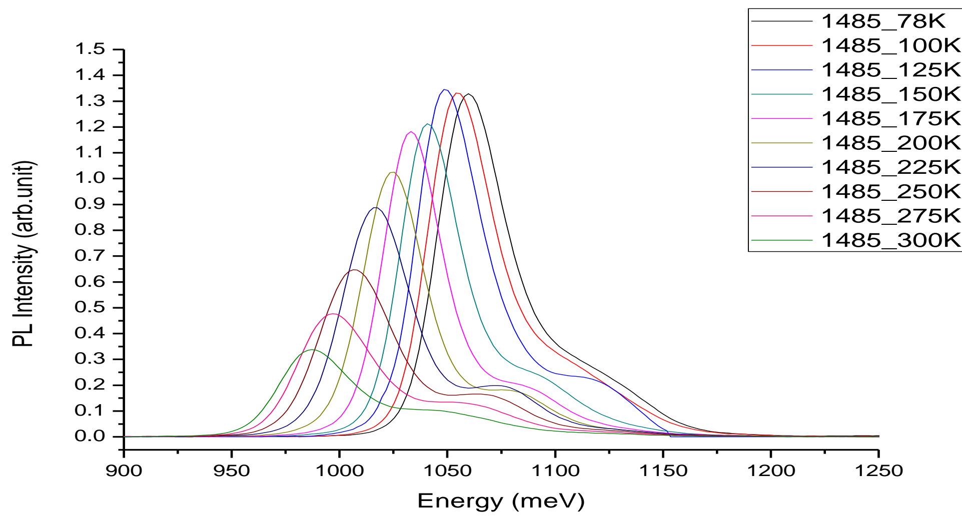

Fig. 6 PL spectra for sample VN1485 at temperatures from 78K to 300K

The spectra show a main peak, with a higher energy (ground state) lower intensity (excited state) shoulder. As temperature is reduced, the spectrum shifts towards the red which is to higher wavelengths. As to the variation of peak emission intensity with temperature, it appears that the peak intensity increases slightly as temperature is increased from 78K, peaking at 125K, before reducing substantially towards 300K.

For purposes of clarity, the spectra in Figure 4.1 were all normalized and plotted in Figure 4.2. It is clear that the spectral main peak red-shifted with reducing of temperature, where at 78K the ground state peak is at 2.24µm and reducing to 1.9µm at 300K. The higher energy shoulder is visible in each spectrum as well.

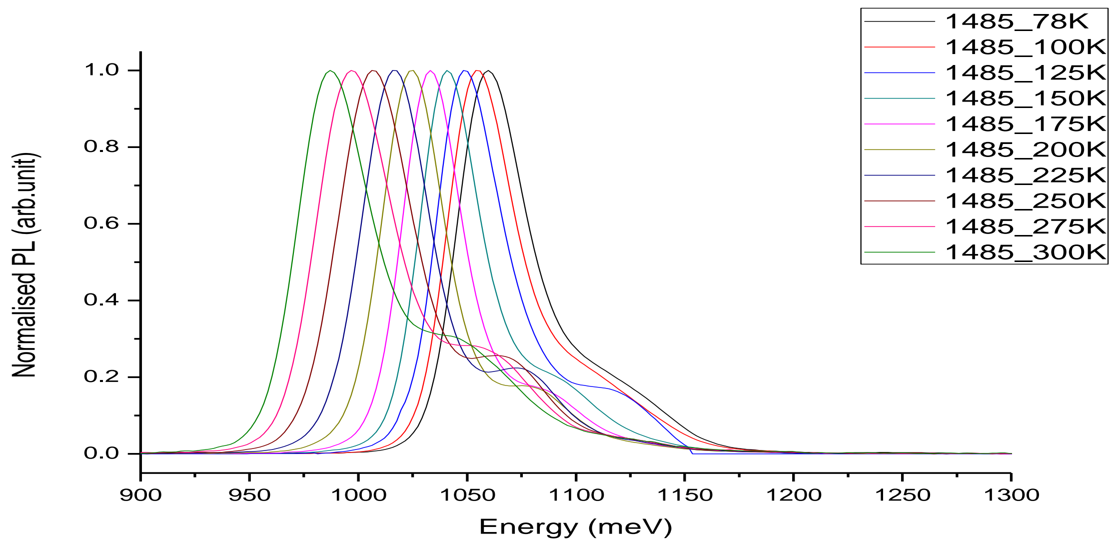

Fig. 7 Normalised PL spectra for sample VN1485 at temperatures from 78K to 300K

To aid in the analysis, the data was fitted to two Gaussian curves (e.g. Figure 4.3, at 225K), the sum of which would account for a main peak and shoulder. The curve fitting tool in OriginLab was applied to the spectral data, with fits made to using fit linear curve. The integrated intensity was then obtained by numerical integration of the Gaussian curves.

At 78K the PL transition energy is found to be 1.14eV from the experimental result, and comparing to the modelling calculation provided by the optoelectronics research group it is assumed that the Ga content, x in the InAs dot is between 30%. The modelling result is based on undoped material only therefore no comparison can be made for the doped sample.

V. CONCLUSION

This paper has presented the mid-wavelength infrared QDIP with 30-layers of DWELLs in the active region where special attention has been given to the optical properties of the intersubband photodetector namely the DWELL detector. The photoluminescence and photocurrent of the device has been investigated.

The results showed impressive results that are good control over the operating wavelength, higher operating temperature and adjustable spectral bias. The DWELL's photoresponse showed a reliance on the applied bias owing to the tilting of the edge of the conductive band and the shift in the probability of tunneling through the obstacles from the Quantum well excited states. By changing the bias it is possible to tune the wavelength window of the detector.

REFERENCES

1. A.Y.Cho. (1971). Film Deposition by Molecular Beam Techniques. Journal of Vaccum Science Technology (8), 31-38.
2. A.Y.Cho. (1979). Recent Developments in structures Molecular Beam Epitaxy (MBE). Journal of Science Technology , 16, 275-284.
3. Broekart, T. P., &Fonstad, C. (1992). Novel Organic Acid Based Etchants for InGaAlAs/InPHeterostructure Devices with AlAs Etch-Stop Layers. Journal of Electrochemical Society , 139 (8).
4. Chang, L., L.Esaki, Howard, W., R.Ludeke, &G.Schul. (1973). Structures Grown by Molecular Beam Epitaxy. Journal of Vacuum Science Technology (10), 655-662.
5. Colorado, U. o. (2010). IR Spectroscopy Tutorial. Retrieved August 25, 2010, from Spectroscopy: http://orgchem.colorado.edu/hndbksupport/irtutor/main.html
6. Gupta, R., Lai, K. T., Missous, M., & Haywood, S. K. (2004). Subbandnonparabolicity estimated from multiple intersubband absorption in highly doped multiple quantum wells. Physical Review B , 69 (3), 033303.
7. Gupta, R., Wong, A. L., & Haywood, S. K. (1999). 3μm intersubband Quantum Well Photodetector (QWIP). Tr. Journal of Physics , 23, 673-679.
8. Haywood, S. K., Lai, K. T., &Missous, M. (2006). Mid-infrared Semiconductor Optoelectronics. Berlin: Springer.
9. Krishna, S. (2005). Quantum dots-in-a-well infrared photodetectors. Journal of Physics D: Applied Physics , 38 (13), 2142-2150.
10. Levine, B. F. (1993). Quantum-well infrared photodetectots. Journal of Applied Physics , 74 (8), 1-81.
11. Ling, H. S., Wang, S. Y., Lee, C. P., & Lo, M. C. (2008). High quantum effieciency dots-in-a-well quantum dot infrared photodetectors with AlGaAs confinement enhancing layer. Applied Physics Letters , 92 (19), 193506.
12. Liu, H. C. (2003). Quantum dot infrared photodetector. Opto-epectronicsReview , 11, 1-5.
13. Martyniuk, P., Krishna, S., &Rogalski, A. (2008). Assessment of quantum dot infrared photodetectors for high temperature operation. Journal of Applied Physics , 104 (3), 034314.
14. Mashade, M. B., Ashry, M., & Nasr, A. (2003). Therotical analysis of quantum dot infrared photodetectors. Semiconductor Science and Technology , 18 (9), 891-900.
15. Micaleff, J., &Wiess, B. L. (1990). The refractive index of III-Iv semiconductor strained-layer superlattices. Optical and Quantum Electronics , 669-684.
16. Osbourn, G. (1982). Journal of Applied Physics. Strained layer superlattices from lattice mismatch materials , 53, 1586-1589.
17. Parker, G. (1994). Introductory Semiconductor Device Physics. Prentice Hall International (UK) Limited.
18. Philips, J. (2002). Evaluation of the fundamental properties of quantum dot infrared detectors. Journal of Applied Physics , 91 (7), 4590-4594.
19. Pryor, C., & Pistol, M. (2005). Bande-edge diagrams for strained III-IV semiconductor quantum wells, wires and dots. Physical Review B , 72, 1098-1121.
20. Rhyzii, V. (1997). Characteristics of quantum well infrared photodetectors. Journal of Applied Physics , 81 (9), 6442-6448.
21. Rinaldi, F. (2002). Annual Report Optoelectronics Department. University of Ulm.
22. Rogalski, A. (2009). Outlook on Quantum dot infrared photodetectors. Optical Memory and Neural Networks (information Optics) , 18 (3), 234-252.
23. Rogalski, A. (2002). Quantum Well Infrared Photoconductors In Infrared Detection Technology. International Journal of High Speed Electronics and Systems, 12 (3), 593-658.
24. Rogalski, A. (2003). Quantum well photodetectors in infrared detector technology. Journal of Applied Physics, 93 (8), 4355-4391.
25. Schneider, H., & Liu, H. C. (2007). Quantum Well Infrared Photodetectors Physics and Applications. Heidelberg: Springer.
26. Shenoi, R. V., Attaluri, R. S., Siroya, A., Shao, J., Sharma, Y. D., Stinz, A., et al. (2008). Low Strain InAs/InGaAs/ quantum dots-in-a well infrared photodetector. Journal Vaccum Science Technology , 26 (3), 1136-1139.
27. Strading, R. A., &Klipstein, P. C. (1990). Growth and characterisation of semiconductors. Bristol: J W Arrowsmith Ltd.
28. Sze, S. M., & Ng, K. K. (2007). Physics Of Semiconductor Devices. John Wiley & Sons.
29. Vurgaftman, I., & Meyer, J. R. (2001). Band parameters for III-IV compound semiconductor and thier alloys. Applied physics review , 89 (11), 5818-5875.
30. Wilson, J., & Hawkes, J. (1998). Optoelectronics an Introduction. Prentice Hall.